J Biorheol (2024) 38(2):55–64
DOI 10.17106/jbr.38.55

ORIGINAL ARTICLE (Special issue on Cellular and Molecular Mechanobiology)

Frequency-dependent characteristics of osteoblast calcium signaling responses to microvibrational stimulation

Katsuya Sato[1,*], Taira Eihara[2]

[1]*Graduate School of Technology, Industrial and Social Sciences, Tokushima University, 2-1 Minami Josanjima, Tokushima city, Tokushima, 770-8506, Japan*
[2]*Graduate School of Sciences and Technology for Innovation, Yamaguchi University, 2-6-1 Tokiwadai, Ube city, Yamaguchi, 755-8611, Japan*

Received: 16 July 2024 / Accepted: 17 September 2024

Abstract The metabolism of bone tissue is regulated by mechanical stimuli. It has been reported that low-intensity, high-frequency vibratory stimuli can activate bone tissue metabolism. Identifying effective vibration conditions that enhance bone formation could potentially be exploited to prevent the onset and progression of osteoporosis, thereby improving quality of life in an aging society. Experiments using model animals have investigated the effects of various frequencies of vibratory stimuli, but there remains no consensus on the most effective frequency. In this study, we used a simple cell culture system to evaluate the calcium signaling response of osteoblasts subjected to micro-vibratory stimuli at different frequencies. Using a custom-developed vibration device, we applied vibratory stimuli to osteoblasts under microscopic observation and evaluated the calcium signaling response using a fluorescent calcium indicator. The vibratory stimuli were applied from 45 to 120 Hz in 15 Hz increments and from 120 to 45 Hz in 15 Hz decrements. The results of the experiment showed that the highest response rate was obtained at 60 Hz in the 45 to 120 Hz group, and at 105 Hz in the 120 to 45 Hz group. These results suggest that in an experimental system where the frequency is swept, the cells respond at the beginning of stimulation, and that habituation may contribute significantly thereafter.

Keywords osteoblast, mechanical vibration, bone metabolism, mechanotransduction, biomechanics

1. Introduction

Bones constitute vital organs that provide support and protection, facilitate blood production, and serve as a crucial reservoir for calcium within the body. Global aging trends have led to an escalating number of people with osteoporosis, posing a societal challenge. In normal bone tissue, a cyclic process of bone metabolism, involving bone formation and resorption, maintains a consistent structure [1]. However, in osteoporosis, a deficiency of estrogen causes excessive bone resorption, resulting in the deterioration of bone microarchitecture [2]. The progression of osteoporosis can lead to complications such as back pain and hip fractures, contributing to a fourfold higher mortality rate among elderly individuals that have osteoporosis compared with those that have not [3, 4].

Artificial enhancement of the bone-forming action in bone metabolism could potentially impede the progression of osteoporosis. Current pharmacological treatments for osteoporosis include estrogen replacement therapy and alendronate administration. However, estrogen replacement therapy has side effects such as breast cancer, endometrial hyperplasia, coronary artery diseases, and venous thromboembolism [5], while alendronate administration is linked to complications including esophageal and oral disorders, gastrointestinal disturbances, and renal dysfunction [6, 7]. To reduce these side effects, non-pharmacological approaches such as physical exercise and strength training are therefore used concurrently with lower doses of medication [8–10].

A potential alternative to pharmacological treatment involves low-magnitude, high-frequency (LMHF) vibrational stimulation. LMHF vibration typically involves acceleration amplitudes below 1 *g*, with vibration frequencies commonly ranging from 20 to 90 Hz. Despite inducing mechanical strains (5–10 με) significantly smaller than those occurring in the skeleton during movement (2000–3000 με), LMHF vibration has been reported to enhance

*E-mail: katsuyas@tokushima-u.ac.jp

bone strength and suppress the reduction in bone mass associated with osteoporosis by promoting bone formation [11–13]. For example, previous studies have reported that the application of LMHF vibratory stimuli to experimental animals improves bone quality, enhances biomechanical properties, and stimulates bone regeneration [14–16]. Additionally, in rat tibiae containing titanium implants, the effects of LMHF loading was shown to depend on the duration of the load, which was applied at fifteen consecutive frequencies (12, 20, 30, ..., 150 Hz) for 2000 cycles each [17].

Experimental investigations using animal models have provided a consensus on the beneficial effects of LMHF vibrational stimulation on promoting bone formation. However, effective conditions of LMHF vibration for bone formation vary among studies, and the underlying mechanisms through which LMHF vibration affects bone metabolism remain unclear. Furthermore, the manner in which bone cells, including osteoblasts responsible for bone formation, respond to the subtle mechanical stimuli of LMHF vibration and the mechanisms through which bone-forming activities are stimulated remain unresolved. The complexity of mutually influencing factors in animal model experiments poses challenges in understanding the mechanism of action of LMHF vibration [18]. Consequently, there is a need to elucidate the response characteristics of osteoblasts to LMHF vibrational stimuli in a simplified cell culture system [19].

This study aimed to elucidate the response characteristics of cultured osteoblasts under varying LMHF vibratory stimuli. Specifically, we investigated the effects of incrementing frequencies (45, 60, 75, ..., 120 Hz), decrementing frequencies (120, 105, 90, ..., 45 Hz) on the intracellular calcium signaling of osteoblasts. Calcium signaling plays a pivotal upstream role in biochemical signaling cascades, regulating various downstream responses such as cell proliferation, alkaline phosphatase activity, and collagen production. Consequently, by observing calcium signal responses, it was possible to evaluate the mechanical stimulus response characteristics (mechanosensitivity) of osteoblasts.

2. Materials and Methods

2.1 Cell culture and fluorescent labeling

The mouse osteoblastic cell line MC3T3-E1 was provided by the RIKEN BioResource Research Center through the National BioResource Project of the Ministry of Education, Culture, Sports, Science and Technology, Japan. Cells were pre-cultured in α-minimum essential medium containing 10% v/v fetal bovine serum and maintained at 37°C in 5% CO_2. Prior to the experiment, 2.5×10^4 cells were seeded on a fibronectin-coated, ϕ 35 mm glass-bottomed dish. After 12 h incubation to enable cell adhesion, the culture medium was replaced with Hank's balanced salt solution (HBSS) containing 10 μM Fluo-4 acetoxymethyl ester (Dojindo Laboratories, Mashiki, Japan) and 0.04% v/v Pluronic F-127 (Life Technologies, Carlsbad, CA, USA), and the culture was then continued for 30 min in the CO_2 incubator to allow intracellular uptake of the dye. The cells were then rinsed twice with Dulbecco's phosphate-buffered saline, fresh was HBSS added, and images of Fluo-4 fluorescence intensity, which is proportional to the intracellular Ca^{2+} concentration, were acquired.

2.2 Vibration loading device and vibration application conditions

Figure 1 shows a photograph of the vibration loading device previously developed in our laboratory [20]. The device is designed to be placed on the stage of an inverted microscope. Two linear sliders attached to the base plate are used to fix the position of the vibration plate, which is connected to a piezoelectric actuator via a jig. A glass-bottomed dish (ϕ 35 mm) is fixed via a urethane sponge to a dish holder installed in the center of the vibration plate. The vibrating plate is reciprocated horizontally by a piezoelectric actuator, subjecting the cells adhered to the glass-bottomed dish to vibration. The piezoelectric actuator (MC-140L; Mess-Tek, Wako, Japan) has an elastic hinge mechanism with a pivoting motion and a stroke of 140 μm. A sinusoidal driving voltage is generated using an Arduino DUE microcomputer and digital-to-analog converter (MCP4725 breakout board; Adafruit Industries, New York, NY, USA) and amplified using a piezoelectric amplifier (M-2502-1; Mess-Tek) to drive the actuator. In this study, the acceleration amplitude was set to 0.2 *g*, and the frequency was either incremented from 45 Hz to 120 Hz in 15 Hz steps (referred to as 45–120 Hz treatment) or decremented from 120 Hz to 45 Hz in 15 Hz steps (referred to as 120–45 Hz treatment). These vibration conditions were determined by referring to those used in previous studies that used animal models [8–11]. The duration of vibrational stimulation at each frequency step was 5 min, with a 30 s interval between each frequency. Vibrational

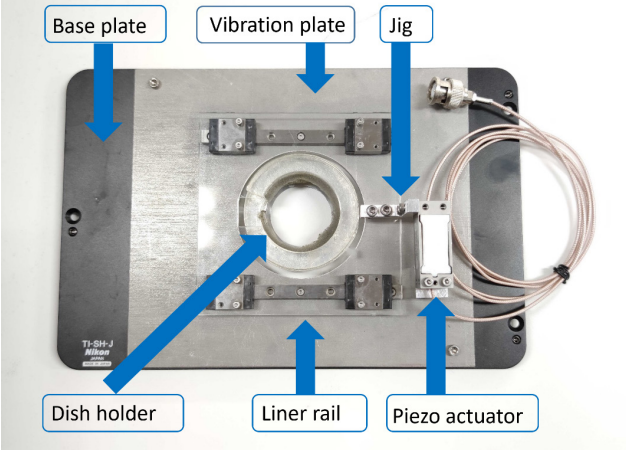

Figure 1 Micro-vibration loading device

stimulation commenced 30 s after the initiation of cell imaging. The total cell observation time was 33 min. As an illustrative example, the timing for the 45–120 Hz treatment is depicted in Figure 2.

2.3 Imaging system and settings

A confocal laser scanning fluorescence microscope (A1R; Nikon, Tokyo, Japan) was used for cell observation. Images were acquired using a 40× dry objective, a 512 × 512 pixel resolution (0.62 μm × 0.62 μm pixel size), and a scan rate of 0.2 fps. A 488 nm laser excitation source and a bandpass filter (central wavelength, 525 nm; bandwidth, 50 nm) were used to image Fluo-4 fluorescence. The observation time for each experiment was 33 min. All experiments were conducted under a normal atmosphere.

2.4 Region of interest and image analysis

Owing to the raster scanning mechanism of the microscope, images of cells subjected to vibration were affected by variable distortions. To simplify the fluorescence imaging analysis, the region of interest (ROI) for measuring the average fluorescence intensity was initially fixed. Figure 3 shows the fluorescence images of the cells before vibration and the same cells during vibration. In this experiment, the intensity of the vibration was kept constant using an acceleration amplitude of 0.2 *g*. Therefore, the displacement amplitude depended on the vibration frequency. A simple ROI was manually traced around the cells, as shown in Figure 3. To maintain a constant ratio of cell and background fluorescence intensities within the ROI for all vibration frequencies, we set the ROI to be 2.5 times the area of the cell before vibration and measured the average fluorescence intensity within the ROI. The temporal change in Fluo-4 fluorescence was affected by photobleaching and several cellular activities, which caused both increases and decreases in fluorescence intensity in individual cells. Therefore, as shown in Figure 4, the raw fluorescence intensities were corrected by subtracting a quadratic fit function from each original curve and normalizing each curve relative its initial intensity.

2.5 Cellular response characteristics and statistical analysis

Figure 5 plots the normalized fluorescence intensities of cells in the control group (n = 26), which were imaged in the absence of vibrational stimulation. The mean value of the peak fluorescence intensity of the cells was 1.101 ± 0.037 (mean ± standard deviation). Therefore, the threshold intensity for determining the presence or absence of a cellular response was set at 1.1, and the cells were judged to have responded when the normalized fluorescence intensity exceeded this value for more than 5 s.

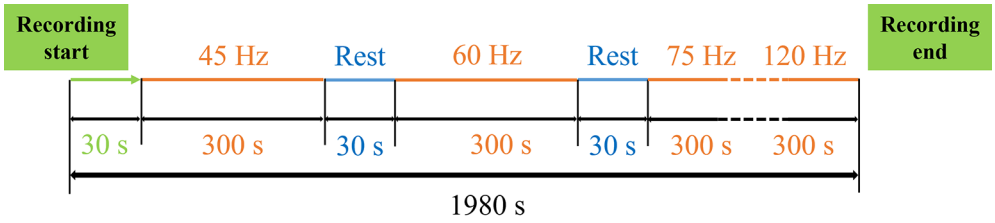

Figure 2 Timetable of recording and vibration application

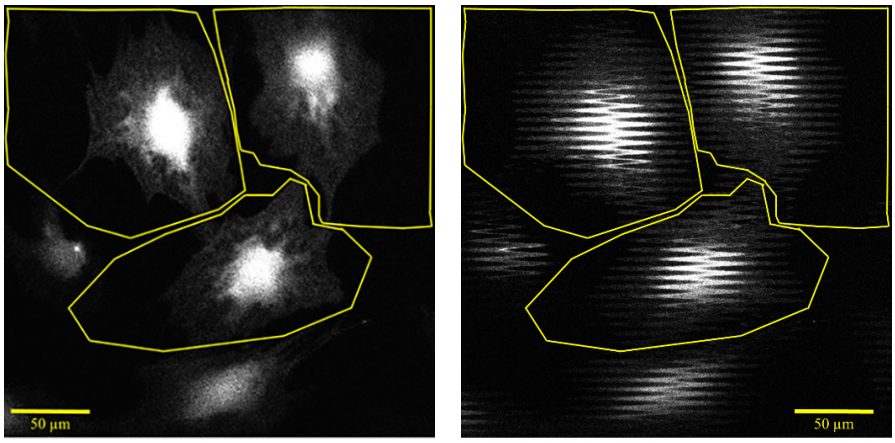

(a) Initial image of cells without vibration (b) Distorted image of cells under vibration

Figure 3 Example of fluorescent image of Fluo 4 loaded cell under vibration stimuli. Due to the image construction principle of scanning microscope, image of cell are distorted. ROIs are set to enclose an entire cell.

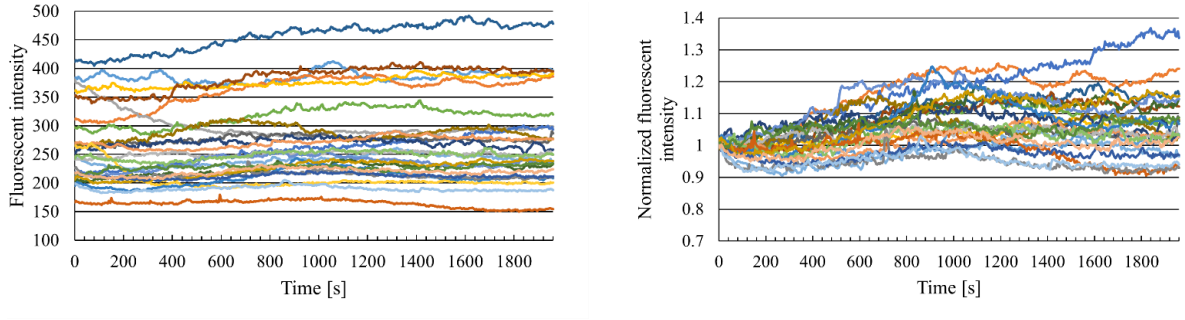

(a) Raw data of fluorescent intensities (b) Corrected and normalized curve

Figure 4 Examples of time course change in fluorescent intensities graph. (a) Raw data of fluorescent intensities. The measured fluorescence intensity data varied between cells and were not uniform. Additionally, they were influenced by medium- to long-term fluctuations. (b) Corrected and normalized curve of fluorescent intensities. By applying correction and normalization, it is possible to extract the changes in fluorescence intensity that are due to transient calcium signaling responses.

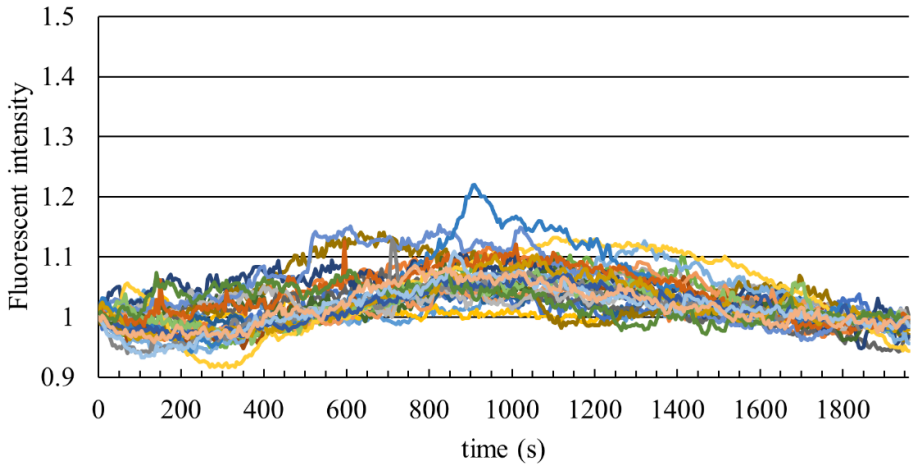

Figure 5 Time course of fluorescence intensity values in the control group. This graph represents the normalized fluorescence intensity values of Fluo 4 in cells that were not subjected to vibration.

The response rate, response intensity, and response duration were used as indices to evaluate the response characteristics of the cells. For each vibration condition, the response rate was defined as the proportion of cells that responded; the response intensity was defined as the mean peak value of the normalized fluorescence intensity of responding cells; and the response duration was defined as the mean time that the normalized fluorescence intensity exceeded the threshold value.

Fisher's exact test was used to statistically analyze the cell response rates. Because the response intensity and response duration did not follow normal distributions under certain conditions, statistical comparisons were made using the non-parametric Kruskal–Wallis test. When significant differences were observed between groups, post-hoc testing was performed using the Steel–Dwass test. The significance level for all tests was set at $P < 0.05$. All statistical analyses were performed using EZR (Saitama Medical Center, Jichi Medical University, Saitama, Japan), which is a graphical user interface for R (The R Foundation for Statistical Computing, Vienna, Austria). More precisely, it is a modified version of R commander designed to add statistical functions frequently used in biostatistics [21].

3. Results

3.1 Calcium signaling response of osteoblasts to the 45–120 Hz treatment

Figure 6 shows representative fluorescence images obtained before (Fig. 6a) and during (Fig. 6b–g) 45–120 Hz treatment, and Fig. 7 shows the corresponding temporal variation in the fluorescence intensity of Fluo-4 in 47 cells. The areas enclosed by the yellow lines in Fig. 6 represent the ROIs, and the pink- and blue-shaded areas in Fig. 7 indicate the vibration and resting periods, respectively.

3.2 Calcium signaling response of osteoblasts to the 120–45 Hz treatment

Figure 8 shows representative fluorescence images

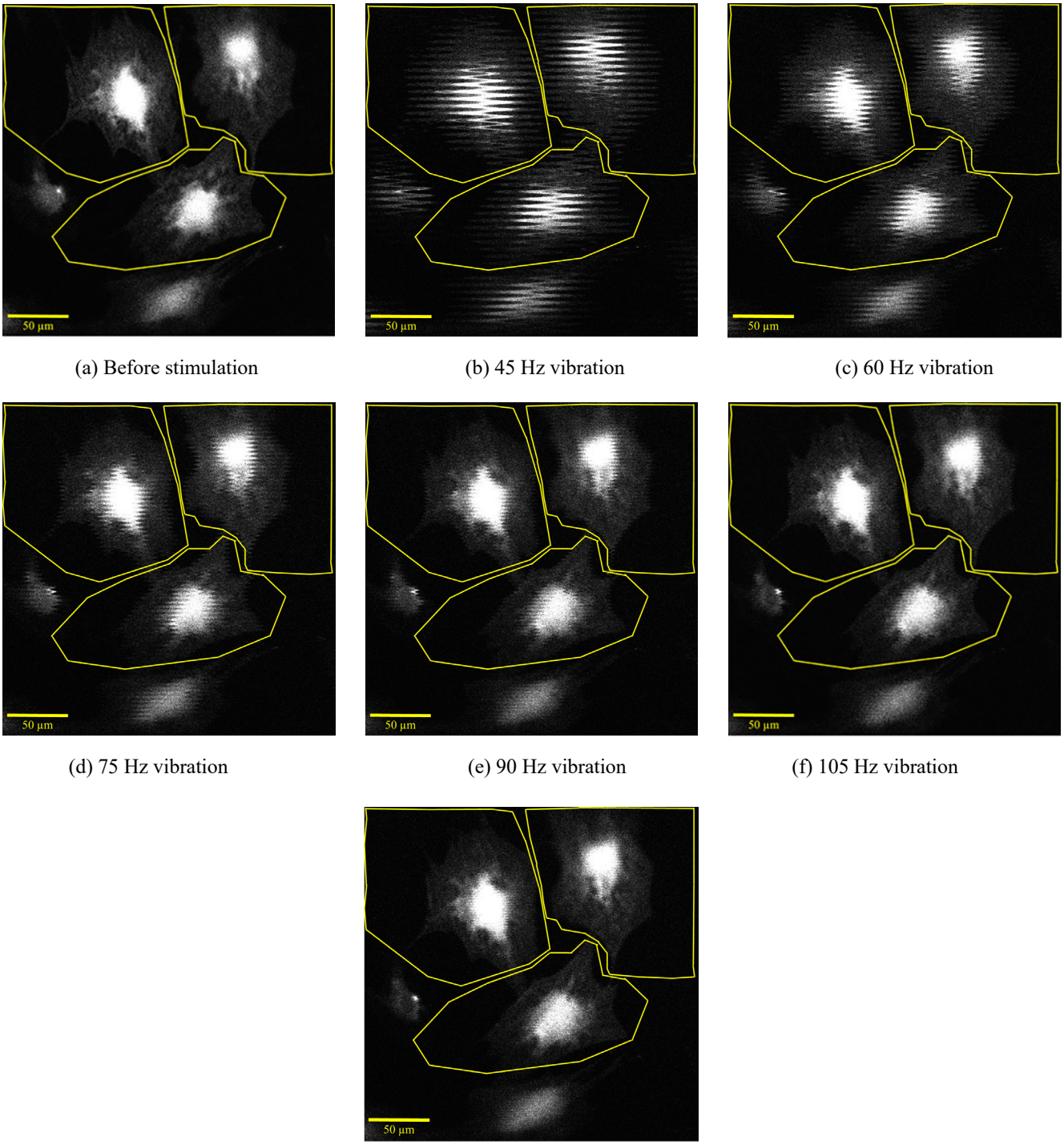

(a) Before stimulation (b) 45 Hz vibration (c) 60 Hz vibration

(d) 75 Hz vibration (e) 90 Hz vibration (f) 105 Hz vibration

(g) 120 HzVibration

Figure 6 An example of Fluo 4 fluorescence observation images in 45 Hz–120 Hz group. Images (a) through (g) correspond to the respective frequencies of the applied vibrations. The regions enclosed in yellow in the images represent the ROI.

obtained before (Fig. 8a) and during (Fig. 8b–g) 120–45 Hz treatment, and Fig. 9 shows the corresponding temporal variation in the fluorescence intensity of Fluo-4 in 38 cells. The areas enclosed by the yellow lines in Fig. 8 represent the ROIs.

3.3 Relationship between cellular response rate and vibration frequency

The vibration frequency-dependent rates of response to 45–120 Hz and 120–45 Hz treatments are shown in Figs. 10 and 11, respectively. For both treatments, Fisher's exact test identified a significant difference in response rates among

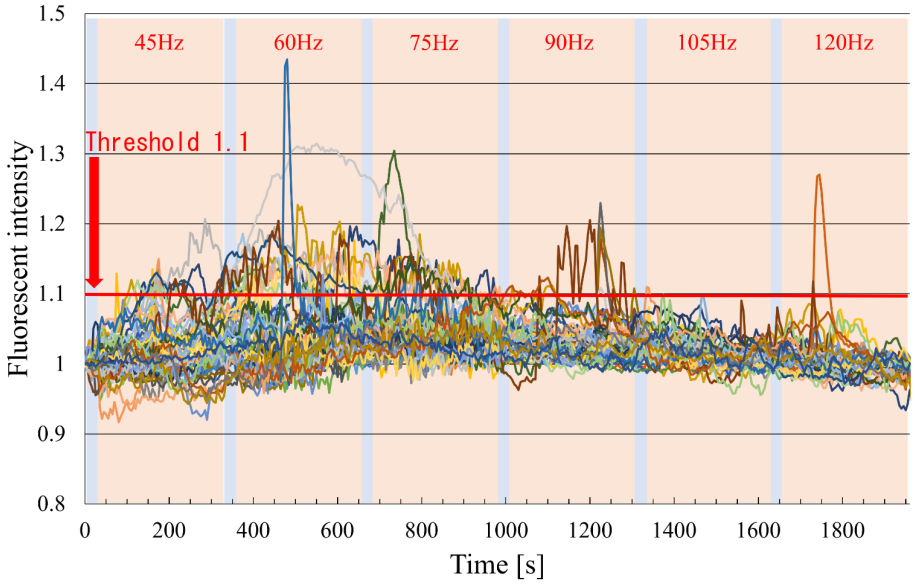

Figure 7 Time course of Fluo 4 fluorescence intensity values in the 45 Hz–120 Hz group. The periods during which each frequency vibration was applied are highlighted in orange. The periods highlighted in light blue represent rest periods during which no vibrations were applied.

cells treated with different vibration frequencies. In the 45–120 Hz group, the response rate was highest at 60 Hz, and the response rates for the frequencies before and after this were also high. In the 120–45 Hz group, on the other hand, the response rate was highest at 105 Hz, and the response rates for the frequencies before and after this were also high. The overall trend in response rates was that the 120–45 Hz group tended to have a higher response rate.

3.4 Relationship between cellular response intensity and vibration frequency

Figures 12 and 13 show vibration frequency-dependence of the average cellular fluorescence intensity in response to 45–120 Hz and 120–45 Hz treatments, respectively. The non-parametric Kruskal–Wallis test identified significant differences within the 45–120 Hz group but none within the 120–45 Hz group. For the 45–120 Hz group, the Steel–Dwass test identified a significant difference in response intensity between the cells stimulated with 45 and 60 Hz vibrations.

3.5 Relationship between cellular response duration and vibration frequency

Figures 14 and 15 show the vibration frequency-dependence of the average duration of cellular responses to 45–120 Hz and 120–45 Hz treatments, respectively. The Kruskal–Wallis test identified significant differences in the response durations among different vibration frequencies for both the 45–120 Hz group and the 120–45 Hz group. In the 45–120 Hz group, the post hoc Steel–Dwass test identified significant differences in response durations between cells stimulated with 45 and 60 Hz vibrations and between cells stimulated with 60 and 90 Hz vibrations. In the 120–45 Hz group, significant differences in response durations were identified between cells stimulated with 120 and 90 Hz vibrations.

4. Discussion

In this study, the highest intracellular calcium concentrations were measured in response to a vibration frequency of 60 Hz in 45–120 Hz group, On the other hand, the 120–45 Hz group had the highest response rate at 105 Hz. Looking at the graphs of frequency and cell response rate, the general shape of the graph is similar for both the 45–120 Hz group and the 120–45 Hz group. In other words, the cells respond from the start of stimulation, and then the cell response subsides, and in the latter half of the observation period, the cells do not respond much. This is thought to reflect the effects of the osteoblast's habituation to mechanical stimulation. Therefore, in the experimental system used in this study, the same cells were given vibration stimuli of different frequencies in sequence, but the effects of habituation in the cells were significant, making it difficult to accurately evaluate the relationship between the response characteristics of osteoblasts and vibration frequency. We thought that by applying vibrations of different frequencies to the same cells, we could eliminate the effects of individual differences between cells, but in reality, the effects of habituation were significant. On the other hand, the overall cell response rate between the 45–120 Hz group and the 120–45 Hz group was higher in the 120–45 Hz group. This result suggests that even when the habituation effect of the cells is taken into account, the cell response rate is higher at 105 Hz than at 60 Hz.

We will consider the habituation effect of cells. In this study, the total time of vibration stimulation to osteoblasts

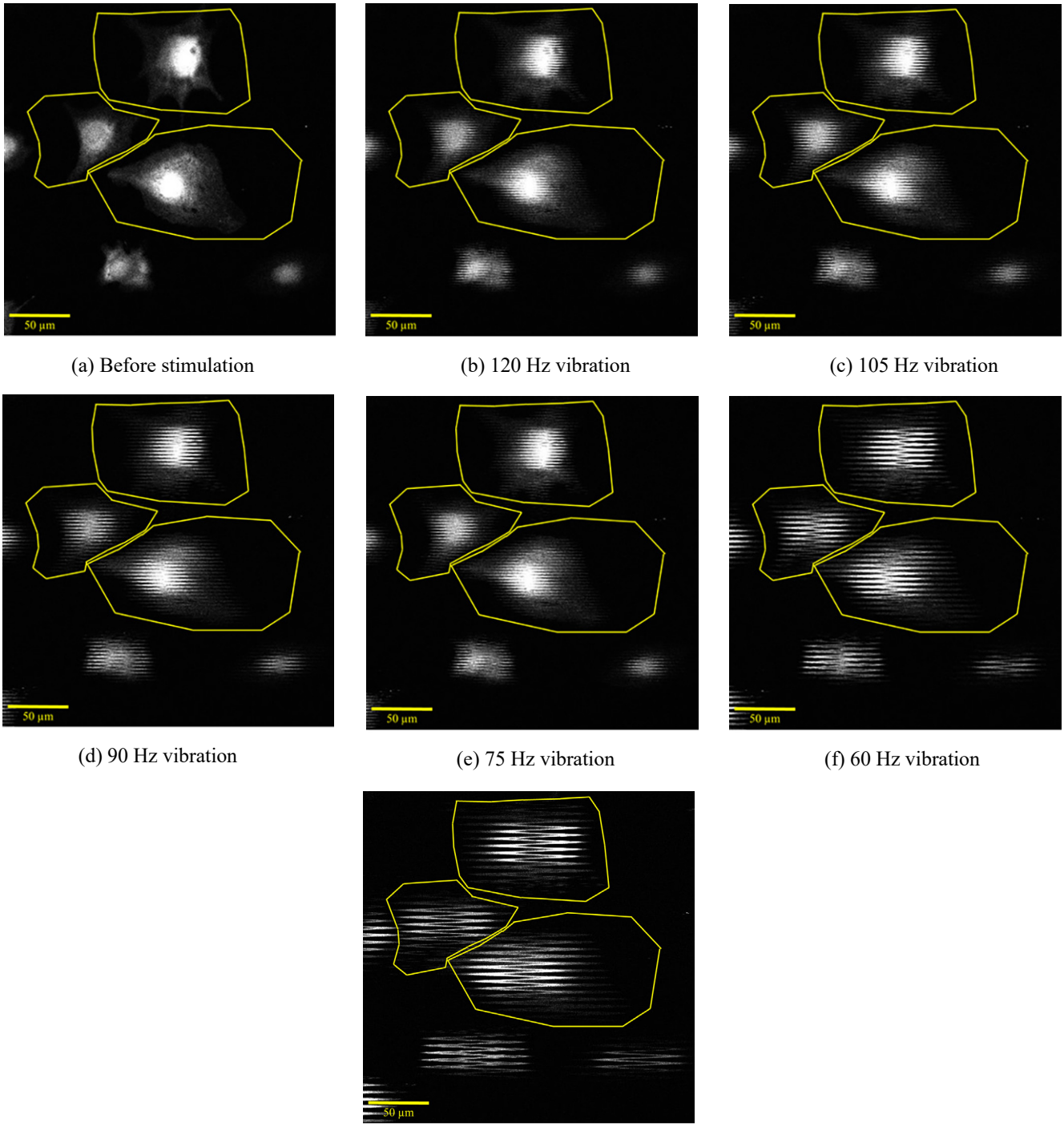

(a) Before stimulation (b) 120 Hz vibration (c) 105 Hz vibration

(d) 90 Hz vibration (e) 75 Hz vibration (f) 60 Hz vibration

(g) 45 Hz vibration

Figure 8 An example of Fluo 4 fluorescence observation images in 120 Hz–45 Hz group. Images (a) through (g) correspond to the respective frequencies of the applied vibrations. The regions enclosed in yellow in the images represent the ROI.

was about 30 minutes. As a result, the response rate decreased due to the habituation effect of cells after about 15 minutes had passed since the start of vibration stimulation. Therefore, when applying vibration stimulation continuously, it is inefficient from the perspective of the habituation of cells to apply stimulation for a long time at a time, and it is thought that a vibration application time of approximately 15 minutes is appropriate.

In this study, the calcium signaling response characteristics of osteoblasts were evaluated using three indices: the proportion of responding cells, the peak response intensity, and the duration of the response. The response rate of the cells was greatly affected by the habituation effect of the cells, and we were unable to obtain results showing that the response rate increased at a specific frequency. However, a significant difference in the peak intensity was only observed in response

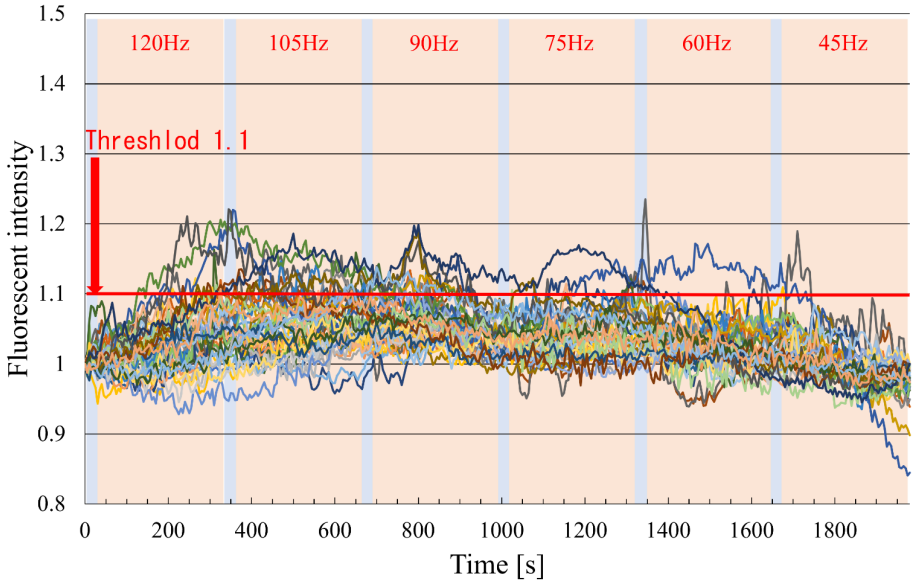

Figure 9 Time course of Fluo 4 fluorescence intensity values in the 120 Hz–45 Hz group. The periods during which each frequency vibration was applied are highlighted in orange. The periods highlighted in light blue represent rest periods during which no vibrations were applied.

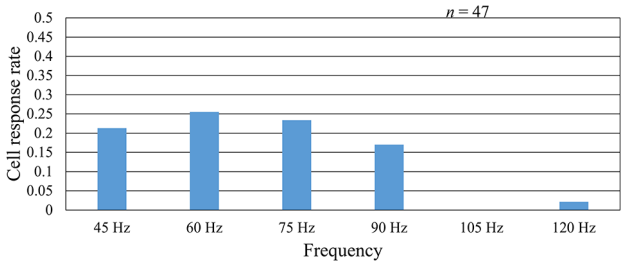

Figure 10 Relation between Cell response rate and vibration frequency in 45 Hz–120 Hz group. Fisher's exact test revealed a significant difference between frequency and cellular response rate. The frequency with the highest response rate was 60 Hz, with frequencies centered around 60 Hz showing high response rates.

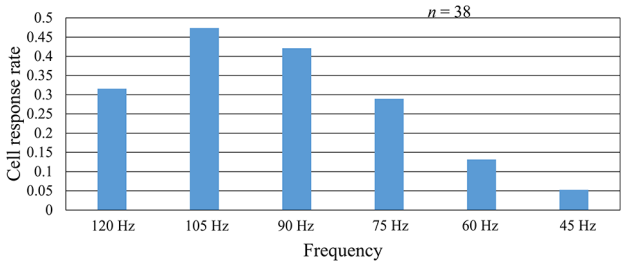

Figure 11 Relation between Cell response rate and vibration frequency in 120 Hz–45 Hz group. Fisher's exact test revealed a significant difference between frequency and cellular response rate. The frequency with the highest response rate was 105 Hz, with frequencies centered around 105 Hz showing high response rates.

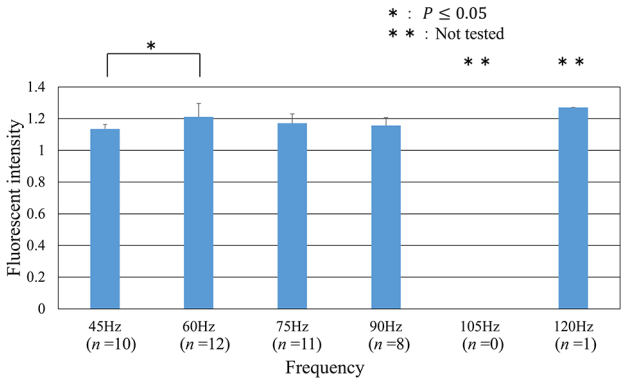

Figure 12 The relationship between average fluorescence intensity and frequency. Due to the low number of responding cells at frequencies of 105 Hz and 120 Hz, statistical testing was not performed for these frequencies. A statistically significant difference was observed only between 45 Hz and 60 Hz.

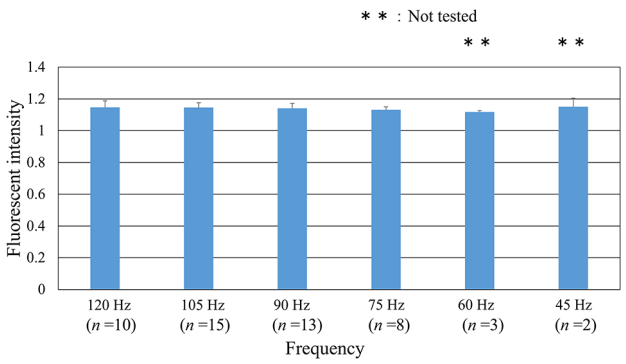

Figure 13 The relationship between average fluorescence intensity and frequency. Due to the low number of responding cells at frequencies of 60 Hz and 45 Hz, statistical testing was not performed for these frequencies. In the 120 Hz–45 Hz group, no statistically significant differences were observed.

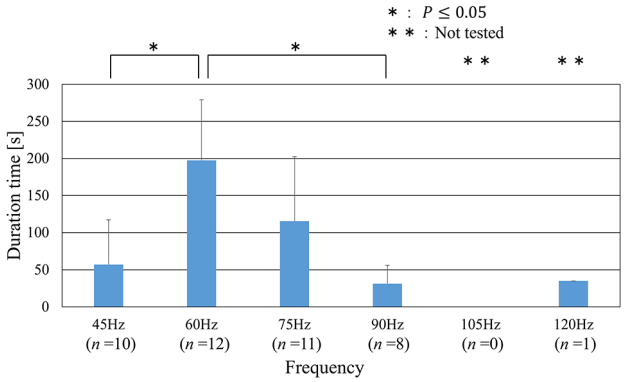

Figure 14 The relationship between response duration and frequency. Due to the low number of responding cells at frequencies of 105 Hz and 120 Hz, statistical testing was not performed for these frequencies. Statistically significant differences were observed between 45 Hz and 60 Hz, and between 60 Hz and 90 Hz. The response duration of the cells was longest at a frequency of 60 Hz.

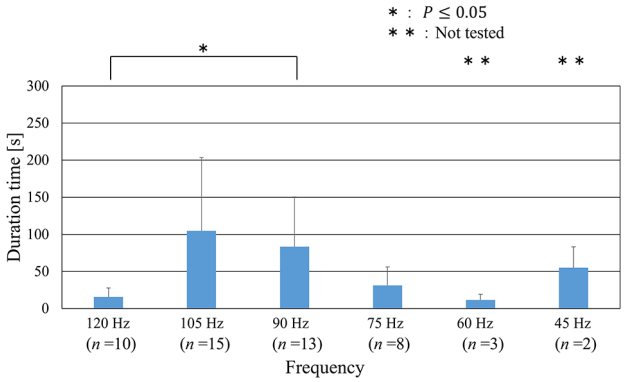

Figure 15 The relationship between response duration and frequency. Due to the low number of responding cells at frequencies of 60 Hz and 45 Hz, statistical testing was not performed for these frequencies. A statistically significant difference was observed only between 120 Hz and 90 Hz.

to frequencies between 45 and 60 Hz when the frequency was incremented, with no differences being observed among other vibration frequencies. No differences in peak response intensities were observed among any frequencies when the vibration frequency was decremented. These results suggest that the response intensity of osteoblasts to microvibrational stimuli are not significantly frequency-dependent. In terms of response duration, the general shape of the graph was similar for the 45–120 Hz and 120–45 Hz groups. However, while the cell response rate was generally higher for the 120–45 Hz group, the response duration was generally longer for the 45–120 Hz group. When you consider that there was almost no difference in response intensity between the two groups, it can be seen that, although the number of responding cells was relatively small in the 45–120 Hz group, the duration of the response of the cells was relatively long.

The mechanosensing mechanism of osteoblasts is poorly understood. We hypothesize that the relatively dense cell nucleus oscillates at a different phase than other intracellular structures, possibly constituting a component of the mechanosensor. The oscillation of the nucleus could induce stretching and deformation of the connected actin cytoskeleton, transmitting forces to focal adhesions. This phenomenon might serve as the mechanosensing mechanism through which cells detect microvibrations. If so, we hypothesize that the nucleus and actin cytoskeleton can be modeled as a vibrational system consisting of a mass, spring, and damper. Future research that utilizes the construction of such a dynamic model may provide useful insights into understanding the response characteristics of osteoblasts to oscillatory stimuli.

During the application of vibrational stimuli, we did not specifically control the flow of the HBSS recording medium in the glass-bottomed dish. Although the intensity of the microvibrational stimulus was assumed to be weak and thus induce minimal liquid flow, such flow was not entirely absent. The natural frequency of the oscillation of the HBSS liquid in the glass bottom dish may have existed as a specific frequency, and this may have affected the results of the experiment. This could result in significant flow of the recording medium at that frequency, potentially exerting shear stress on the cells. Investigating the influence of liquid flow (e.g., by adding microbeads to the recording medium and observing their flow during microvibrational stimulation) remains an important future task. In order to verify this possibility, it may be necessary to perform the same experiment using glass-bottom dishes of different sizes. Additionally, it is possible that the natural frequency of the experimental apparatus itself. In that case, it would be necessary to verify the reproducibility of the results by conducting similar experiments using devices with different designs and structures from those used in this study.

In this study, we used three indices to evaluate the characteristics of the calcium signal response of osteoblasts: cell response rate, response intensity, and response duration. Various response evaluation indices have been proposed for calcium signaling, including intensity, frequency, number of repetitions, and interval time, and the response characteristics that these indices characterize are referred to as calcium signaling fingerprints [22–24]. The results of this study showed that the effect of cell habituation was significant in terms of the cell response rate, and it was not possible to reach a definite conclusion. But on the other hand, there was no frequency dependence in terms of response intensity. In terms of response duration, it was suggested that 60 Hz was longer than 105 Hz when comparing the two. However, the relationship between these obtained cell response characteristics and the actual osteoblast bone formation activity is still unclear. What response characteristics are important for activating osteoblast bone formation? Unfortunately, it is difficult to obtain findings from this study alone, and we hope to see progress in a wide range of research, including everything from upstream to downstream of osteoblast signaling.

5. Conclusion

In this study, we evaluated the calcium signaling response of osteoblasts to LMHF stimuli applied at different frequencies. The results showed that the effect of cell acclimation was significant in terms of the cell response rate, and it was not possible to determine that a specific frequency was effective. Regarding response duration, when comparing 60 Hz and 105 Hz, there is a possibility that 60 Hz is relatively longer. In contrast, the frequency dependence of the intensity of the calcium signaling response was minimal. In addition, the effects of habituation in the cells were observed in this study. As a result, it was found that the appropriate duration of vibration stimulation per session was approximately 15 minutes.

These experimental results provide insights into the effective frequency conditions for efficiently stimulating osteoblasts. Additionally, these findings may offer clues for understanding the mechanosensory mechanisms of osteoblasts in response to LMHF stimuli, which remain largely unexplored.

Acknowledgements This study was supported by the Support Center for Advanced Medical Sciences, Tokushima University Graduate School of Biomedical Sciences and partly funded by a Grant-in-Aid for Scientific Research (KAKENHI) from the Japan Society for the Promotion of Science (grant number 24K1570100). We thank Edanz (https://jp.edanz.com/ac) for editing a draft of this manuscript.

References

1. Matumoto T, Inoue D. Journal of the Japan Geriatrics Society. 1998; 35(4): 599–604. (in Japanese)
2. Tilman DR, Sundeep K, Lorenz CH. Osteoporosis: now and the future. The Lancet. 2011; 377: 1276–87.
3. Hinoi E, Arai K. YAKUGAKU ZASSHI. 2019; 139: 13–4. (in Japanese)
4. Miura M, Sato Y. YAKUGAKU ZASSHI. 2019; 139: 27–33. (in Japanese)
5. Yager DJ, Davidson EN. Estrogen carcinogenesis in breast cancer. The New England Journal of Medicine. 2006; 354: 270–82.
6. Kelly R, Taggart H. Incidence of gastrointestinal side effects due to alendronate is high in clinical practice. BMJ. 1997; 315: 1231–7.
7. Gonzalez-Moles AM, Bagan-Sebastian VJ. Alendronate-related oral mucosa ulcerations. Journal of Oral Pathology & Medicine. 2002; 29(10): 514–8.
8. Tezval M, Biblis M, Sehmisch S, Schmelz U, Kolios L, Rack T, Stuermer MK, Stuermer KE. Improvement of femoral bone quality after low-magnitude, high-frequency mechanical stimulation in the ovariectomized rat as an osteopenia model. Calcified Tissue Internataional. 2011; 88: 33–40.
9. Rubin C, Recker R, Cullen D, Ryaby J, McCabe J, McLeod K. Prevention of postmenopausal bone loss by a low-magnitude, high-frequency mechanical stimuli: a clinical trial assessing compliance, efficacy, and safety. Journal of Bone and Mineral Research. 2009; 19(3): 343–51.
10. Hwang SJ, Lublinsky S, Seo Y-K, Kim IS, Judex S. Extremely small-magnitude accelerations enhance bone regeneration: a preliminary study. Clinical Orthopaedics and Related Research. 2009; 467: 1083–91.
11. Xie L, Jacobson MJ, Choi SE, Busa B, Donahue RL, Miller ML, Rubin TC, Judex S. Low-level mechanical vibrations can influence bone resorption and bone formation in the growing skeleton. Bone. 2006; 39: 1059–66.
12. Ward K, Alsop C, Caulton J, Rubin C, Adams J, Mughal Z. Low magnitude mechanical loading is osteogenic in children with disabling conditions. Journal of Bone and Mineral Research. 2009; 19(3): 360–9.
13. Ozcivici E, Luu YK, Adler B, Qin Y-X, Rubin J, Judex S. Mechanical signals as anabolic agents in bone. Nature Reviews Rheumatology. 2010; 6: 50–9.
14. Gilsanz V, Wren AL Tishya, Sanchez M, Dorey F, Judex S, Rubin C. Low-level, high-frequency mechanical signals enhance musculoskeletal development of young women with low BMD. Journal of Bone and Mineral Research. 2006; 21: 1464–74.
15. Matsumoto T. KAKEN database, (2011-04-01–2014-03-31).
16. Matsumoto T, Itamochi S, Hashimoto Y. Effect of concurrent use of whole-body vibration and parathyroid hormone on bone structure and material properties of ovariectomized mice. Calcified Tissue Internataional. 2016; 98: 520–9.
17. Ogawa T, Zhang X, Naert I, Vermaelen P, Deroose MC, Sasaki K, Duyck J. The effect of wholebody vibration on peri-implant bone healing in rats. Clin Oral Implants Res. 2011; 302–7.
18. Rubin TC, Sommerfeldt WD, Judex S, Qin Y. Inhibition of osteopenia by low magnitude, high-frequency mechanical stimuli. Drug Discovery Today. 2001; 6: 848–58.
19. Christiansen AB, Matthew JS. The effect of varying magnitudes of whole-body vibration on several skeletal sites in mice. Annals of Biomedical Engineering. 2006; 34: 1149–56.
20. Sato K, Daiki O. Development of vibration mechanical stimuli loading device for live cell fluorescence microscopy. Journal of Biomechanical Science and Engineering. 2022; 17(2). DOI: 10.1299/jbse.21-00294
21. Kanda Y. Investigation of the freely-available easy-to-use software "EZR" (Easy R) for medical statistics. Bone Marrow Transplant. 2013; 48: 452–8.
22. Godin LM, Suzuki S, Jacobs CR, Donahue HJ, Donahue SW. Mechanically induced intracellular calcium waves in osteoblasts demonstrate calcium fingerprints in bone cell mechanotransduction. Biomechanics and Modeling in Mechanobiology. 2007; 6: 391–8.
23. Li L, Stefan MI, Novere NL. Calcium input frequency, duration and amplitude differentially modulate the relative activation of calcineurin and CaMKII. PLOS One. 2012; 7(9): e43810.
24. Smedler E, Uhlen P. Frequency decoding of calcium oscillations. Biochimica et Biophysica Acta. 2014; 1840: 964–9.